

Supporting Information

The Benefits of the ZnO/Clay Composite Formation as a Promising Antifungal Coating for Paint Applications

Eva de Lucas-Gil ¹, Javier Menéndez ², Laura Pascual ³, José F. Fernández ¹ and Fernando Rubio-Marcos ^{1,4,*}

¹ Electroceramic Department, Instituto de Cerámica y Vidrio, CSIC, Kelsen 5, 28049 Madrid, Spain; elucas@icv.csic.es (E.d.L.-G.); jfernandez@icv.csic.es (J.F.F.)

² Encapsulae, S.L., Lituania, 10, 12006 Castellón de la Plana, Spain; jmenendez@asepticae.com

³ Instituto de Catálisis y Petroleoquímica, CSIC, Marie Curie 2, 28049 Madrid, Spain; laura.pascual@icp.csic.es

⁴ Escuela Politécnica Superior. Universidad Antonio de Nebrija. C/Pirineos, 55, 28040 Madrid, Spain

* Correspondence: fmarcos@icv.csic.es

1.- Size Modification Process of the Micrometric ZnO via Chemical Route

The starting ZnO morphology is reflected in **Figure S1a**. As can be seen, the predominant structure consists of hexagonal prisms with lengths of 1-2 μm . Likewise, another nearly hexagonal smaller particles are present in the morphological set. This is because the hexagonal morphology is typical of ZnO well-defined crystals. The structural characterization of the reaction intermediate product generated during the synthesis process (marked in red colour) compared to ZnO precursor (signalled in black colour) are performed by X-ray diffraction (XRD). **Figure S1b** shows diffraction peaks of the reaction intermediate product that match to hydrozincite structure hydrozincite, $\text{Zn}_5(\text{CO}_3)_2(\text{OH})_6$. Finally, the experimental details are schematically shown in **Figure S1c**.

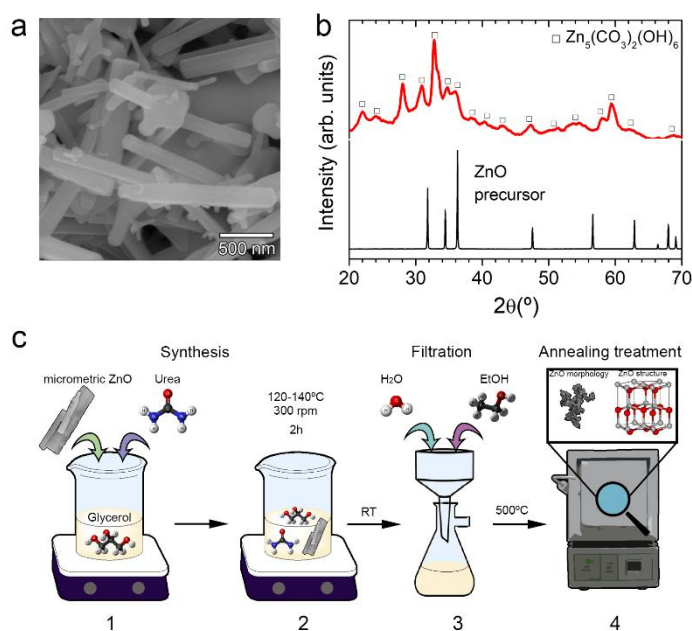


Figure S1. | (a) SEM micrograph shows hexagonal prismatic and nearly hexagonal smaller particles between structures more common of starting ZnO. Scale bar 500 nm. (b) X-ray diffraction patterns of the reaction intermediate product with hydrozincite structure (red) generated during the synthesis process compared to ZnO precursor pattern (black). (c) Scheme of the synthesis process of the nanoparticulated ZnO; (1) Addition of micrometric zinc oxide (6 wt.%) and urea (3.6 mol) to glycerol (3.6 mol), under stirring at room temperature. (2) The resulting solution was heated in an oil bath at 120–140°C and stirred at 300 rpm for 2h at atmospheric pressure. (3) Cooling to room temperature the solution, filtration and washed with water and ethanol several times to remove impurities. (4) The reaction intermediate product (that is, hydrozincite phase) was thermally treated at 500°C for a short time, 5 min, in the air.

2.-. Structural and Morphological Characterization of the Nanoparticulated ZnO

The structural characterization of obtained ZnO is performed by X-ray diffraction (XRD) and Fourier transform infrared spectroscopy (FTIR). **Figure S2a** displays the XRD pattern of obtained ZnO compared with hexagonal wurtzite structure ZnO (JCPDS Card No. 36-1451). As shown, the position and intensity of the diffraction peaks match between them. So, this fact confirms the synthesis of ZnO in a hexagonal wurtzite structure. The FTIR spectrum shows different IR band groups (**Figure S2b**). The IR band at 437 cm^{-1} is ascribed to vibration Zn–O modes. The band group from 1630 to 860 cm^{-1} is associated with different stretching modes of carbonate groups. The broad IR band at 3470 cm^{-1} is typical of O–H stretching mode ($\nu(\text{OH})$) of absorbed water. Additionally, morphological characterization of synthesized ZnO by FE-SEM (**Figure S2c**) shows nanoparticles' agglomerates with a heterogeneous distribution and irregular forms. The image analysis of the nanoparticles displays the average size to 56 ± 8 nm (**Figure S2d**). A close study of a nanoparticle is shown in **Figure S2e**. The determination of particle lattice spacing of ~ 1.630 Å is indexed as the ZnO (110) plane according to JCPDS Card No. 79-0206. This result supports the phase assignment of the ZnO phase by XRD in **Figure S2a**.

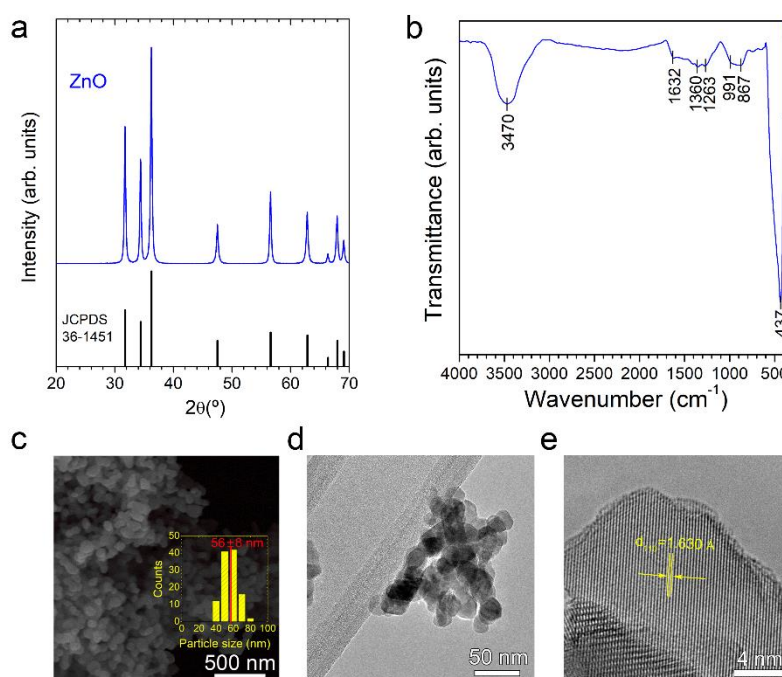


Figure S2. | Structural and Morphological characterization of Nanoparticulated ZnO. (a) XRD pattern and (b) FTIR spectrum corresponding to nanoparticulated ZnO. (c) A generic study by FE-SEM shows the morphology of obtained ZnO. Additionally, inside of the panel c, is indicated the particle size distribution of obtained ZnO, having 56 nm in mean size. In TEM micrographs, it can be

evidenced by the nanometric character of obtained ZnO forming agglomerates (**d**) and the lattice spacing of the ZnO nanoparticles (**e**).

3.- XRD pattern of modified bentonite clay

Figure S3 displays the XRD pattern of modified bentonite clay. As shown, the clay consists mainly of bentonite (JCPDS Card No. 003-0019). Also, the presence of cristobalite as an impurity (JCPDS Card No. 039-1425) is detected.

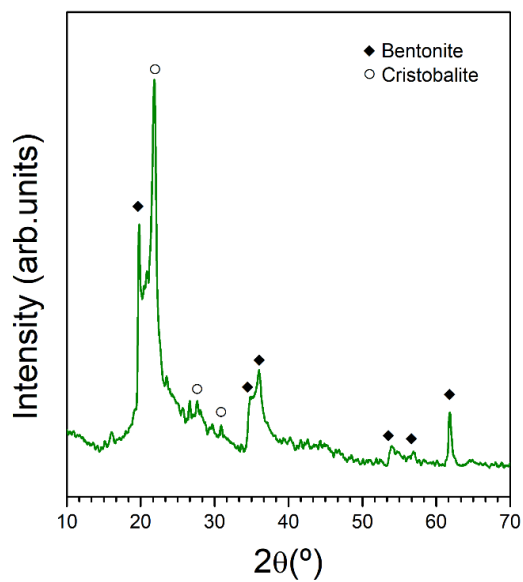


Figure S3. | XRD pattern of modified bentonite clay.

4.- Morphological characterization of inorganic composite precursors.

The morphological characterization of inorganic composite precursors is performed by scanning electron microscopy, SEM. The modified clay (**Figure S4a**) is composed of layers or plates about 2 μm of size and ca. 100 nm of thickness, that is compacted. On the other hand, the morphology of ZnO synthesized is represented in **Figure S4b**. The main morphology of ZnO is small pseudo-spherical particles with sizes of 50-60 nm.

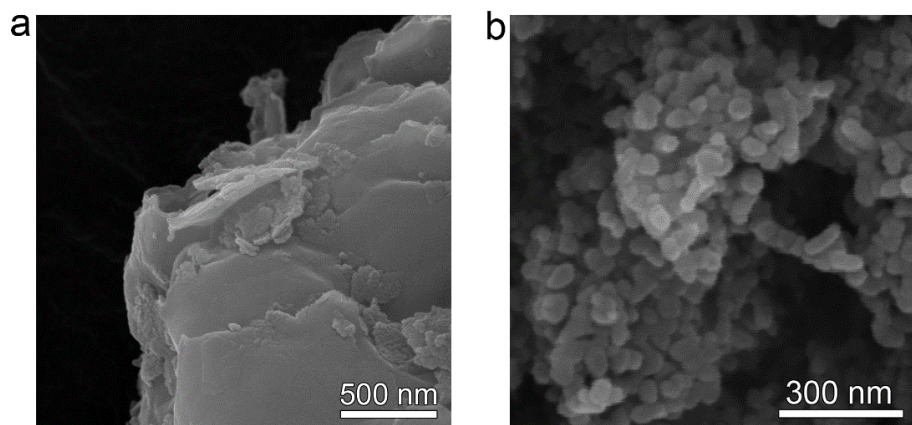


Figure S4. | Morphological characterization of inorganic composite precursors. FE-SEM micrographs of modified clay (**a**) and ZnO obtained (**b**).

5. - Replicas of Bauer-Kirby disk diffusion assay in the paint matrix

To test the efficacy of ZnO paint against fungi, three experiments were performed. As shown in **FigureS5**, the results of the replicas are similar in fresh paint and in dry paint.

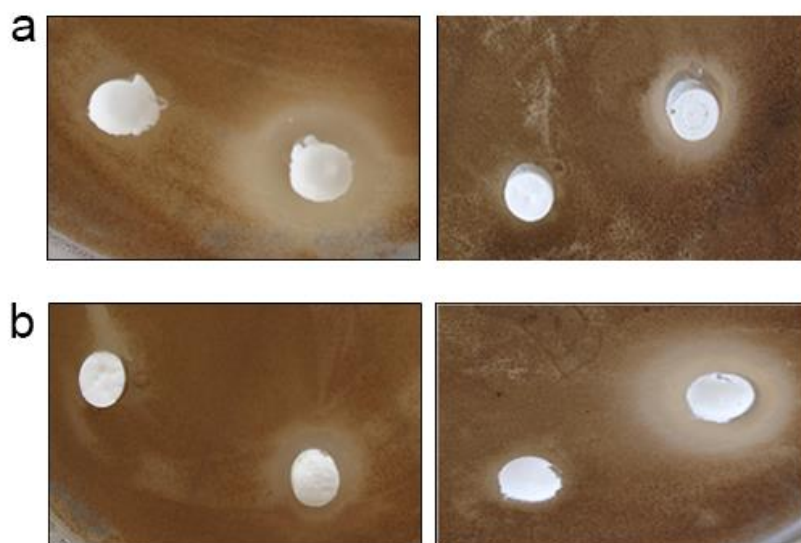


Figure S5. | Bauer-Kirby disk diffusion assay of ZnO/Clay composite against *A. niger*. (a) Experiments of fresh paint and fresh paint with ZnO/Clay. (b) Assay replica of dry paint and dry paint with ZnO/Clay.